Hindawi Publishing Corporation
EURASIP Journal on Image and Video Processing
Volume 2007, Article ID 65184, 9 pages
doi:10.1155/2007/65184

Research Article

Automatic Eye Winks Interpretation System for Human-Machine Interface

Che Wei-Gang,[1] Chung-Lin Huang,[1,2] and Wen-Liang Hwang[3]

[1] *Department of Electrical Engineering , National Tsing-Hua University, Hsin-Chu, Taiwan*
[2] *Department of Informatics, Fo-Guang University, I-Lan, Taiwan*
[3] *Institute of Information Science, Academic Sinica, Taipei, Taiwan*

Received 2 January 2007; Revised 30 April 2007; Accepted 21 August 2007

Recommended by Alice Caplier

This paper proposes an automatic eye-wink interpretation system for human-machine interface to benefit the severely handicapped people. Our system consists of (1) applying the support vector machine (SVM) to detect the eyes, (2) using the template matching algorithm to track the eyes, (3) using SVM classifier to verify the open or closed eyes and convert the eye winks into a sequence of codes (0 or 1), and (4) applying the dynamic programming to translate the code sequence to a certain valid command. Different from the previous eye-gaze tracking methods, our system identifies the open or closed eye, and then interprets the eye winking as certain commands for human-machine interface. In the experiments, our system demonstrates better performance as well as higher accuracy.

1. INTRODUCTION

Recently, there has been an emerging community of machine perception scientists focusing on automatic eye detection and tracking research. It can be applied for vision-based human-machine interface (HMI) applications such as monitoring human vigilance [1–6] and assisting the disable [7, 8]. The eye detection and tracking approaches can be classified into two categories: CCD camera-based approaches [1–11] and active IR-based approaches [12–15].

An eye-wink control interface [7] is proposed to provide the severely disabled with increased flexibility and comfort. The eye tracker [2] makes use of a binary classifier with a dynamic training strategy and an unsupervised clustering stage to efficiently track the pupil (eyeball) in real time. Based on optical flow and color predicates, the eye tracking [4] can robustly track a person's head and facial features. It classifies the rotation of all viewing directions, detects eye blinking, and recovers the 3D gaze of the eyes. In [5], the eye detection operates on the entire image, looking for regions that have the edges with a geometrical configuration similar to the expected one of the iris. It uses the mean absolute error measurement for eye tracking and a neural network for eyes validation.

The eye movement collection data can be analyzed to determine the pattern and duration of eye fixations and the sequence of scan path as a user visually moves his eyes. The eye tracking researches, such as the eye-gaze estimation [2, 9] and eye blink rate analysis [3–5], can be applied to analyze the fatigue and deceit of human being [6]. Another application such as head-mounted goggle type eye detection device [10] with a liquid crystal display is developed for investigation of eye movements of neurological disease patients. In [11], they formulate a probabilistic image model and derive optimal inference algorithms for finding objects. It requires the likelihood-ratio models for object versus background, which can be applied to find faces and eyes on arbitrary images.

The active approaches [12–15] make use of IR devices for the purposes of pupil tracking based on the special bright pupil effect. This is a simple and very accurate approach to pupil detection using the differential infrared lighting scheme. By combining imaging by using IR light and object recognition techniques, the method proposed in [14] can robustly track eyes even when the pupils are not very bright due to significant external illumination interference. The eye detection and tracking process is based on the support vector machine (SVM) and mean shift tracking. Another method [15] exhibits robustness to light changes and camera defocusing. It is capable of handling sudden changes between IR and non-IR light conditions, without changing parameters.

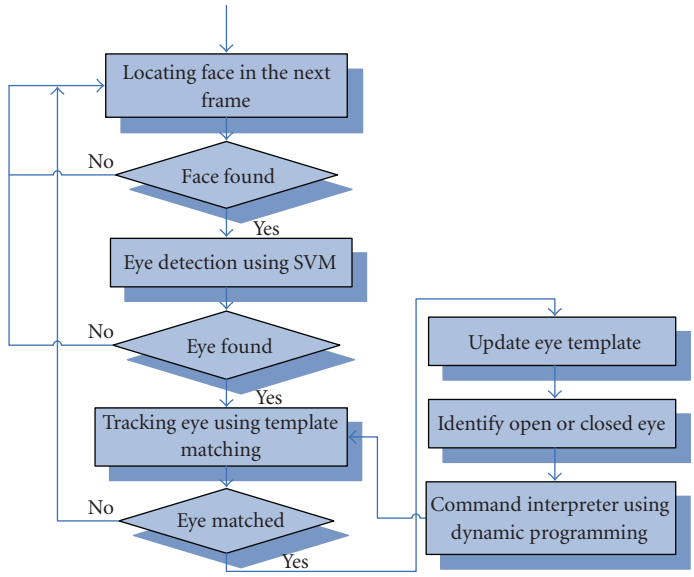

Figure 1: Flowchart of the eye-winks interpretation system.

However, the active methods [12–15] require additional resources in the form of infrared sources and infrared sensors. Here, we propose a vision-based eye-wink control interface for helping the severely handicapped people to manipulate the household devices. Recently, many researchers have shown great interests in the research topics of HMI. In this paper, we propose an eye-wink control HMI system which allows the severely handicapped people to control the appliances by using their eye winks. We assume that the possible head poses of the handicapped people are very limited. Under the front-pose assumption, we may easily locate the eyes, track the eyes, and then identify the open or closed eye.

Before eye tracking, we use the skin color information to find the possible face region which is a convex region larger than a certain size. Once the face region is found, we define the possible eye region in which we may apply SVM to localize the eyes precisely and create the eye template obtained from the identified eye image. In the next frame, we apply the template matching to track the eyes based on the eye template extracted in the previous frame. The eye template is updated every time the eye is successfully tracked. After eye tracking, we apply SVM to verify whether the tracked block is an eye or a noneye region. If it is an eye region, then we use SVM again to identify whether it is an open eye or a closed eye, and then convert the eye winks to a sequence of 1 or 0 codes. Finally, we apply the dynamic programming to validate the code sequence and convert the code sequence into a certain command. The flow chart of the proposed system is illustrated in Figure 1.

2. EYE DETECTION AND TRACKING

Our eye detection and tracking method consists of three stages: (1) face region detection, (2) eye localization, and (3) eye tracking. The three steps are illustrated in the following sections.

2.1. Face region detection

To reduce the eye search region, we need to locate the possible face region. In the captured human face images, we assume that the color distribution of the human face is somehow different from that of the image background. Pixels belonging to face region exhibit similar chrominance values within and across people of different ethnic groups [16]. However, the color of face region may be affected by different illuminations in the indoor environment. For skin color detection, we analyze the color of the pixels in HSI color space to decrease the effect of illumination changes, and then classify the pixels into face color or nonface color based on their hue component only.

Similar to [17], we analyze the statistics of skin color and nonskin color distributions from a set of training data to obtain the conditional probability density functions of skin color, and nonskin color. From 100 training close-up face images, we have the probability density function of hue value H, which can be either face color and nonface color (i.e., $p(H—face)$ and $p(H—nonface)$). Based on hue statistics, we use the Bayesian approach to determine the face color region. Each pixel is assigned to the *face* or *nonface* class that gives the minimal cost when considering cost weightings on the classification decisions. The classification is performed by using the Bayesian decision rule which can be expressed as: if $p(H—face)/p(H—nonface) > \tau$, then the pixel (with H hue value) belongs to a face region, otherwise it is inside a nonface region, where $\tau = p(nonface)/p(face)$. After applying the Bayesian classification on another 100 testing close-up face images, we find that the hue values of 99% of the correct classified facial pixels are within the range [0.175, 0.285].

After the face pixel classification, we cluster these pixels into face color regions. A merging stage is then iteratively performed on the set of homogeneous face color pixels to provide a contiguous region as the candidate face area. Constraints of shape and size of face region are applied on each candidate face area for potential face region detection. Figure 2(a) is the original face image, and Figure 2(b) illustrates the corresponding hue distribution in a 3D coordinate. The face color is distributed in a specified range (in *blue*), and the z-axis shows the normalized hue value (between 0 and 1). To determine the face region, we perform the vertical and horizontal projections on the classified face pixels and find the right and left region boundaries where the projecting value exceeds a certain threshold. The extracted face region is shown in Figure 2(c). We use 100 images of different subjects, background complexities, and lighting conditions to test our face detection algorithm. The correct face detection rate is 88%. The system does not know whether the identified face region is accurate or not, however, if the following eye detection can not locate an eye region, then the detected face region is not a false alarm.

After the face region detection, there may be more than one face-like region in the block image. We select the maximum region as the face region. We assume that eyes should be located in the upper half face area. Once the face region is found, we may assume that the possible eye region is the upper portion of the face region (i.e., the yellow rectangle as shown in Figure 2(d)). These eyes are searched within the yellow rectangle area only.

2.2. Eye localization using SVM

The support vector machine (SVM) [18] is a general classification scheme that has been successfully applied to find a separating hyperplane by maximizing the margin between two classes, where the margin is defined as the distance of the closest point in each class to the separating hyperplane. Given a data set $\{x_i\}_{i=1}^{N}$ of examples with labels $y_i \in \{-1, +1\}$, we find the optimal hyperplane by solving a constrained optimization problem using quadratic programming, where the optimization criterion is the width of the margin between the classes. The separating hyperplane can be represented as a linear combination of the training examples and classifying a new test pattern x by using the following expression:

$$f(x) = \sum_{i=1}^{N} \alpha_i y_i k(x, x_i) + b, \tag{1}$$

where $k(x, x_i)$ is a kernel function and the sign of $f(x)$ determines the class membership of x. Constructing the optimal hyperplane is equivalent to finding the nonzero α_i. Any data point x_i corresponding to nonzero α_i is termed "support vector." Support vectors are the training patterns closest to the separating hyperplane. A training process is developed to determine the optimal hyperplane of the SVM.

The efficiency of SVM classification is based on the selected features. Here, we convert the eye edge image block as the feature vector. An eye edge image is represented by a feature vector consisting of the edged pixel values. We manually select the two classes: positive set (eye) and negative set (noneye). The eye images are processed by using histogram equalization and their image sizes are normalized to 20×10. Figure 3 shows the training samples consisting of open eye images, closed eye images, and noneye images.

Supervise learning algorithms (such as SVM) require as many training samples as possible to reach higher accuracy rate. Since we do not have so many training samples, the alternative way is to retrain the classifier by reusing the missclassified testing samples as the training samples. Here, we have tested at least one thousand unlabeled samples, and then we select the misslabeled data for retraining the classifier. After applying this retraining process, based on the misslabeled data, several times, we can boost the accuracy of the SVM machine.

The eye detection algorithm will search every candidate image block inside the possible eye region to locate the eyes. Each image block is processed by Sobel edge detector and converted to a feature vector consisting of edge pixels, which is more insensitive to the intensity change. With the feature vector (with dimension 200), the image block will be classified by the SVM as an eye block or a noneye block.

2.3. 3 Eye tracking

Eye tracking is applied to find the eye in each frame by using template matching. Given the detected eyes in the previous frame, the eyes in subsequent frames can be tracked frame by frame. Once the eye is correctly localized, we update the eye templates (gray level image) for eye tracking in the next frame. The search region in the next frame is defined by extending 50% length in four directions of the previously located eye bounding box. We individually normalize an eye template as a 20×10 block so that we may track different size eye images which are normalized for template matching. We consider an eye template $t(x, y)$ located at (a, b) of the image frame $f(x, y)$. To compute the similarity between the candidate image blocks and the eye template, we have the following equation as

$$M(p, q) = \min \left[\sum_{x=0}^{w} \sum_{y=0}^{h} | f_n(x + p, y + q) - t_n(x, y) | \right], \tag{2}$$

where (1) w and h are the width and height of the eye template $t_n(x, y)$ and (2) p and q are offsets of the x-axis and y-axis, that is, $a - 0.5^*w < p < a + 0.5^*w$ and $b - 0.5^*h < q < b + 0.5^*h$. If $M(p', q')$ is the minimum value within the search area, the point (p', q') is defined as the best matched position of the eye, and (a, b) is updated by the new position (p', q') as $(a, b) = (p', q')$. The new eye template is applied for the eye tracking in the next frame.

People sometimes blink their eyes unintentionally that may cause error propagation in the template matching process and make the eye tracking fail. Here, we estimate the centroid of the eye in the following frame for the template matching process. To find the centroid, we apply Otsu algorithm [18] to convert the tracked eye image to a binarized image. In the open eye image, the pupil and iris pixels (which are darker) can be segmented as shown in Figure 4(b). The

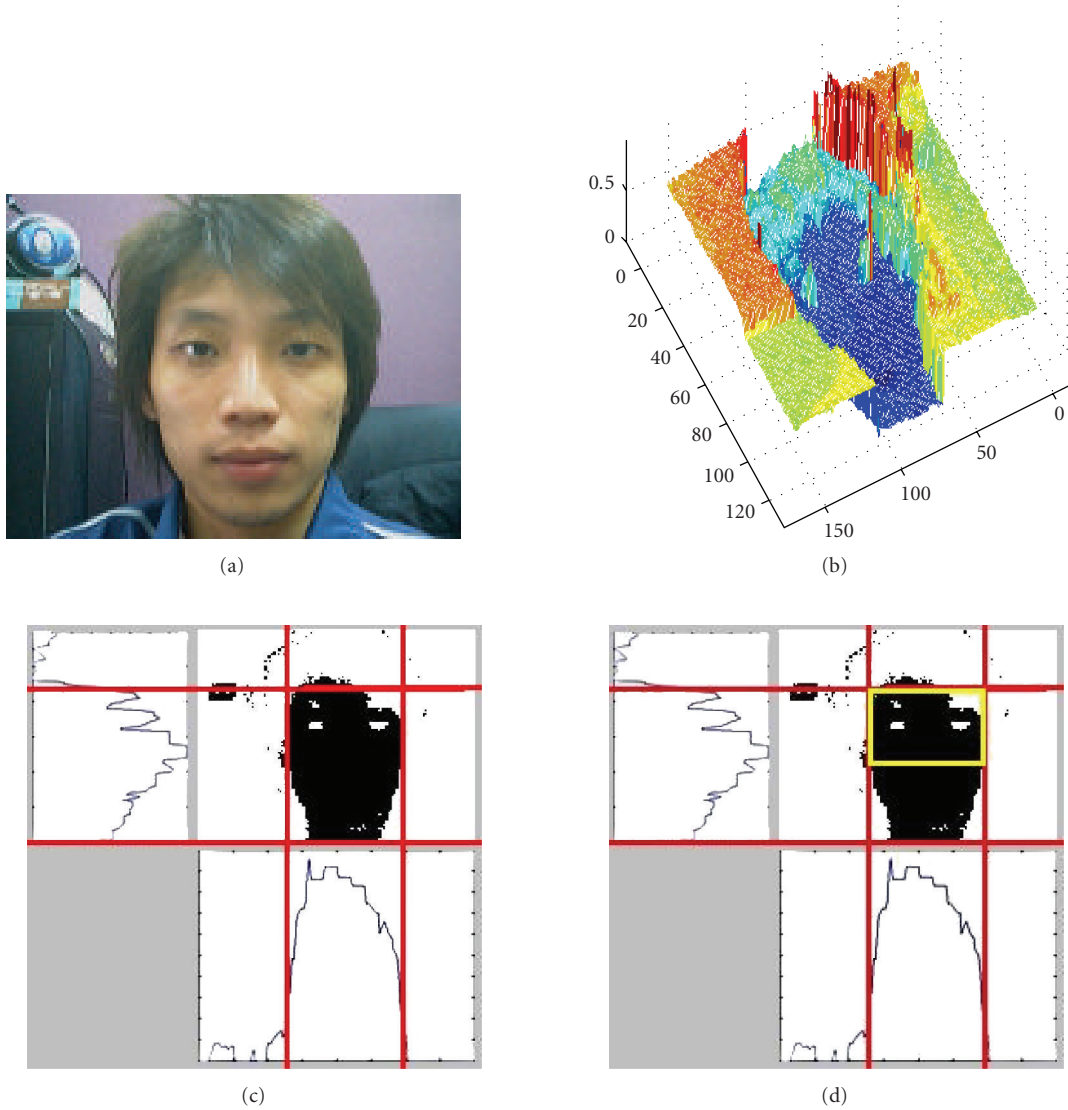

Figure 2: Results of face detection. (a) The original image. (b) Hue distribution of the original image. (c) Skin color projection. (d) Possible eye region.

centroid of iris and pupil is the centroid of the eye region which is located at the center of bounding box. However, in the closed eye image, the centroid is located at the center of eyelashes instead of the center of bounding box. Based on the centroids of the binarized images, the eye tracking will be faster and more accurate. Once the eye region is tracked, we apply the SVM again to classify the tracked region as an open eye, a closed eye, or a noneye region. If the tracked image is a non-eye region, the system will restart the face and eye localization procedures.

3. THE COMMAND INTERPRETER USING DYNAMIC PROGRAMMING

After eye tracking, we continue using SVM to distinguish between the open eye and the closed eye. If the eye opens and exceeds a fixed duration, then it represents a digit "1". Similarly, the closed eye represents a digit "0". So we can convert the sequence of eye winks to a sequence of 0 and 1. The command interpreter validates the sequence of codes, and issues the corresponding output command. Each command is represented by the corresponding sequence of codes. Starting from the base state, the user issues a command by a sequence of eye winks. The base state is defined as an open eye for a long time without intentionally closing the eye. The input sequence of codes is then matched with the predefined sequence of codes by the command interpreter.

To avoid an unintentional or very short eye wink, we require that the duration of a valid open or closed eye should exceed a duration threshold θ_{tl}. If the time interval of the continuously open or closed eye is longer than θ_{tl}, then it can be converted to a valid code, that is, "1" or "0". However, we may allow two contiguous "1" or "0", so we define another threshold $\theta_{th} \approx 2\theta_{tl}$. If the time interval of the

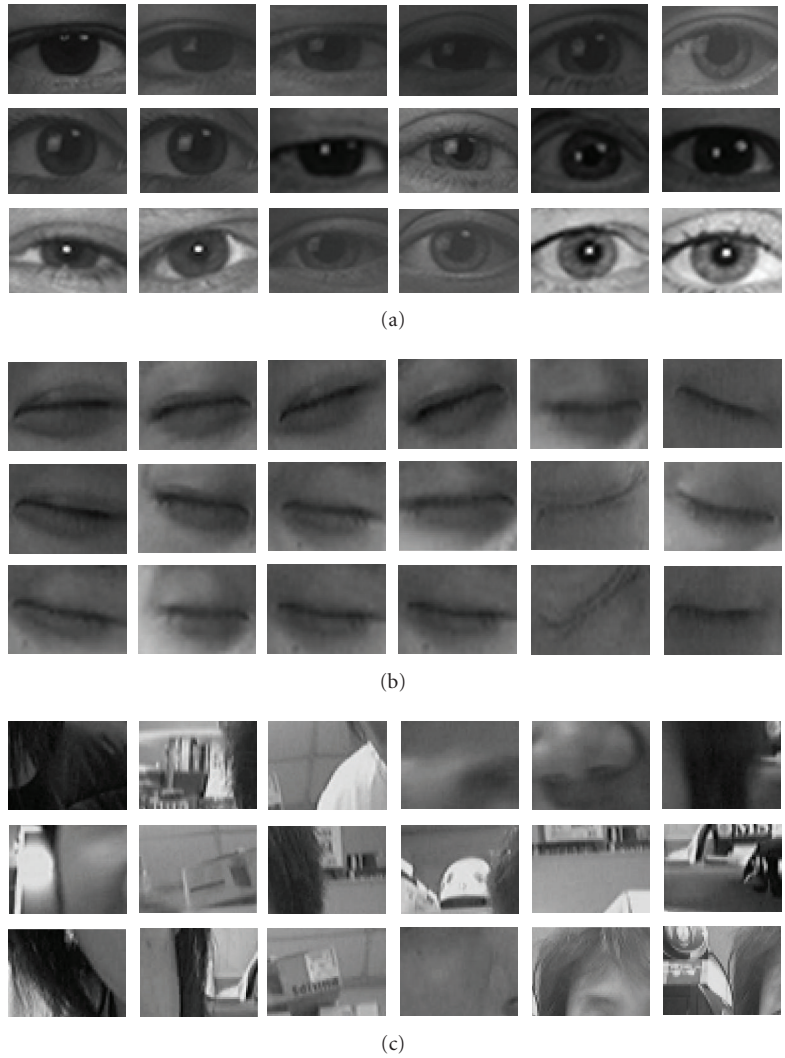

(a)

(b)

(c)

Figure 3: (a) The open eye images. (b) The closed eye images. (c) The noneye images.

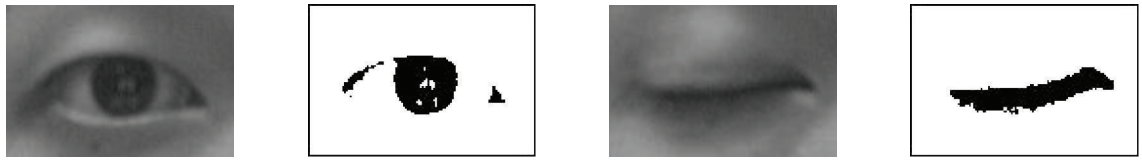

(a) (b) (c) (d)

Figure 4: . (a) The original open eye. (b) The binarized open eye. (c) The original closed eye. (d) The binarized closed eye.

continuously open or closed eye is longer than θ_{th}, then we may consider it as code 00 or 11. The threshold θ_{tl} is user-dependent, user may select the best suitable threshold for his specific eye blinking condition.

Here, we may predefine some valid code sequences, and each one corresponds to a specific command. Once the code sequence has been issued, we need to validate the code sequence. To find a valid code sequence, we need to calculate the similarity (or alignment) score between the issued code sequence and the predefined code sequences. Because the code lengths are different, we need to align the two code sequences to maximize the similarity by using the dynamic programming [19]. We assume the predefined codes as shown in Table 1.

A dynamic programming algorithm consists of four parts: (1) a recursive definition of the optimal score, (2) a dynamic programming matrix for remembering optimal scores, (3) a bottom-up approach of filling the matrix, and

Table 1: Code sequences.

Code length	1	3	4	5
—	0	010	0010	00100
—	—	—	0100	00110
—	—	—	0110	01010
—	—	—	—	01100

(4) a trace back of the matrix to recover the structure of the optimal solution that generates the optimal score. These four steps are explained as follows.

3.1. Recursive definition of the optimal alignment score

There are only three conditions that the alignment can possibly be: (i) residues x_M and y_N are aligned with each other; (ii) residue x_M is aligned to a gap character and y_N appears somewhere earlier in the alignment; or (iii) residue y_N is aligned to a gap character and x_M appears earlier in the alignment. The optimal alignment will be the most preferred of these three cases. The optimal alignment score of the prefix of sequence $\{x_l, \ldots, x_M\}$ to the prefix of sequence $\{y_l, \ldots, y_N\}$ is defined as

$$S(i,j) = \max \begin{cases} S(i-1, j-1) + \sigma(x_i, y_j), \\ S(i-1, j) + \gamma, \\ S(i, j-1) + \gamma, \end{cases} \tag{3}$$

where $i \le M$ and $j \le N$ Case (i) is the score $\sigma(x_M, y_N)$ for aligning x_M to y_N plus the score $S(M-1, N-1)$ for an optimal alignment of everything else up to this point. Case (ii) is the gap penalty γ plus the score $S(M-1, N)$. Case (iii) is the gap penalty γ plus the score $S(M, N-1)$. The divide-and-conquer approach breaks the problem into independently optimized pieces, as the scoring system is strictly local to one aligned column at a time. For instance, the optimal alignment of $\{x_1, \ldots, x_{M-1}\}$ to $\{y_1, \ldots, y_{N-1}\}$ is unaffected by adding the aligned residue pair x_M and y_N. The initial score $S(0, 0)$ for aligning nothing to nothing is zero.

3.2. The dynamic programming matrix

For the pairwise sequence alignment algorithm, the optimal scores $S(i, j)$ are tabulated in a two-dimensional matrix, with $i = 0 \ldots M$ and $j = 0 \ldots N$, as shown in Figure 5. As we calculate the solutions to subproblems $S(i, j)$, their optimal alignment scores are stored in the appropriate (i, j) cell of the matrix.

3.3. A bottom-up calculation to get the optimal score

the dynamic programming matrix $S(i, j)$ is laid out, it is easy to fill it in a bottom-up way, from the smallest problems to progressively bigger problems. We know the boundary conditions in the leftmost column and the topmost row (i.e., $S(0, 0) = 0; S(i, 0) = \gamma^* i$; and $S(0, j) = \gamma^* j$). For example, the optimum alignment of the first i residues of sequence x to nothing in sequence y has only one possible solution which is to align to the gap characters and pay i gap penalties. Once we have initialized the top row and left column, we can fill in the rest of the matrix by using the recursive definition of $S(i, j)$. So we may calculate any cell based on the three adjoining cells to the upper left $(i - l, j - l)$, above $(i - l, j)$, and to the left $(i, j - l)$ which are already known. We may iterate two nested loops, $i = l \ldots M$ and $j = l \ldots N$, to fill in the matrix left to right and top to bottom.

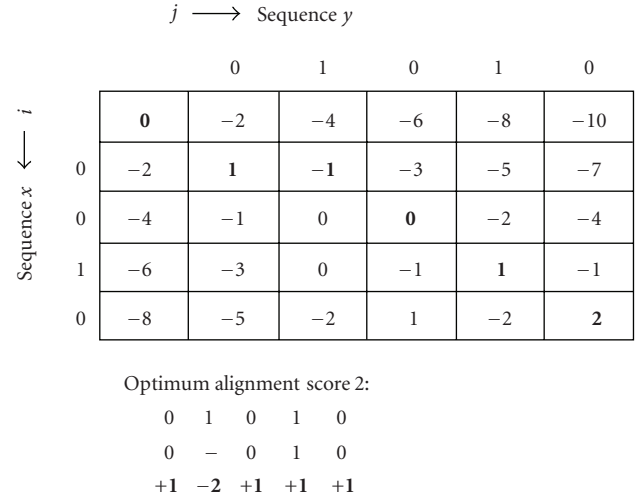

Figure 5: An example of the dynamic programming matrix.

Table 2: Result of eye tracking.

	Video 1	Video 2	Video 3	Video 4
Total frame #	1763	1544	583	1241
Tracking failure frame #	17	19	6	15
Correct rate	99 %	98.7 %	98.9 %	98.7 %
Average correct rate			98.8 %	

3.4. A trace back to get the optimal alignment

Once we have finished filling the matrix, the score of the optimal alignment of the complete sequences is the last score, that is, $S(M, N)$. We still do not know the optimal alignment; however, we recover this by a recursive trace back of the matrix. Starting from cell (M, N), we determine which of the three cases (*i.e.*, (3)) can be applied to record that choice as part of the alignment, and then follow the appropriate path for that case back into the previous cell on the optimum path. We keep doing that, one cell in the optimal path at a time, until we reach cell (0, 0), at which point, the optimal alignment is fully reconstructed. Figure 5 shows an example of the dynamic programming matrix for two code sequences, $x = 0010$ and $y = 01010$ (0: closed eye, 1: open eye). The scores of match, mismatch, and insertion or deletion are +1, −1, and −2, respectively. The optimum path consists of the cells marked by red rectangles.

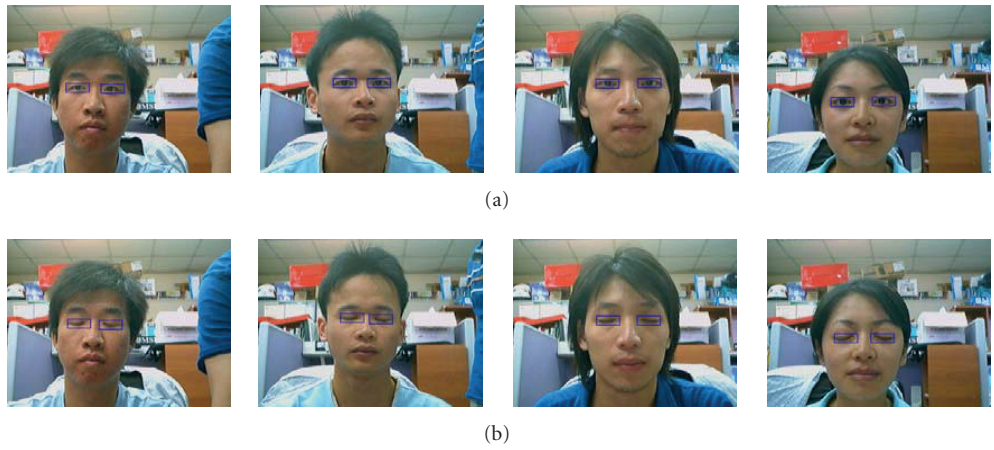

(a)

(b)

Figure 6: (a) Open eyes, and (b) closed eyes detected correctly.

Table 3: Results of eye signal detection.

	User #1	User #2	User #3	User #4
Command 1	29/30	25/27	18/18	35/38
Command 2	15/15	13/13	5/7	15/17
Command 3	13/13	15/18	12/13	18/20
Command 4	14/15	10/12	6/7	14/17
Command 5	13/15	16/17	10/11	18/20
Command 6	17/17	14/19	8/8	6/8
Command 7	17/19	17/19	10/12	10/12
Command 8	18/21	18/21	13/13	21/25
Command 9	16/17	8/10	6/8	17/18
Correct rate	95 %	90.7%	90.6%	88%
Average correct rate			90.1 %	

4. EXPERIMENT RESULTS

We use a Logitech QuickCam Pro3000 camera to capture the video sequence of the disable, and the image resolution is 320×240. The system is implemented on a PC with Athlon 3.0 GHz CPU with Microsoft Windows XP. The eye-wink control system can achieve the speed of 13 frames per second. We have tested 5131 frames of the videos of four people under normal indoor lighting conditions. Based on the SVM for eye detection, the accuracy of the eye detection inside the correctly detected face region is above 90%. The correct classification rate of the open and closed eye is also higher than 92%. Figure 6 shows that the SVM-based eye classifier can correctly identify the open and closed eyes. The SVM classifier works fine under different illumination conditions due to the intensity normalization of the training images via histogram equalization. The face region is separated into the two parts for the detection of the individual left eye and the right eye.

Table 2 lists the results of eye tracking applied on four different test videos. "Total frames #" indicates the total number of frames in each video. "Tracking failure frame #" is the number of frames in which the eye tracking fails. The eye tracking fails when the system can not locate the eye accurately, and then it may missidentify the open eye as a closed eye or vice versa. The correct rate of eye tracking is defined as

$$\text{correct rate} = \frac{\text{Total frame \#} - \text{Tracking failure frame}}{\text{Total frame \#}} \quad (4)$$

Table 2 shows that the proposed system achieves 98% correct eye identification.

Table 3 shows the results of eye-winks interpretation system operating on the test video sequences of four different users. Our system can interpret nine different commands. Each command is composed of a sequence of eye winks. For each command, the correct interpretation rate for a different user is described in terms of r_1/r_2, where r_2 is the total test video sequences for the specific command issued by the designated user, and r_1 indicates the correctly identified video sequences.

Figure 7 shows our system eye-wink control interface. The red solid circle indicates that the eyes are open. Similarly, the green solid circle indicates that the eyes are closed. There are nine blocks at the right portion. In each block, there is a binary digit number representing the specific command code. In the base mode, we design eight categories: medical treatments, a diet, a TV, a radio, anair conditioner, a fan,

(a)

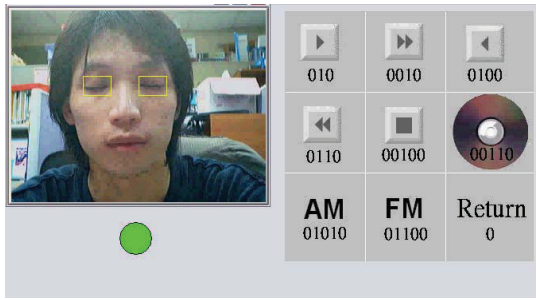

(b)

Figure 7: Program interface. (a) Layer 1 commands. (b) Layer 2 commands for audio.

a lamp, and a telephone. There are two layers in the command mode, so we can create at most 9*9(81) commands. Here, we only use 8*8 + 1(65) commands because in each layer, we have a "Return" command. In Figure 7, we illustrate layer 1 commands and layer 2 commands.

5. CONCLUSION AND FUTURE WORK

We propose an effective algorithm for eye-wink interpretation for human-machine interface. By integrating SVM and dynamic programming, the eye-wink control interpretation system will enable the severely handicapped people to manipulate the household appliances by using a sequence of eye winks. Experimental results have illustrated the encouraging performance of the current methods in both accuracy and speed.

REFERENCES

[1] P. W. Hallinan, "Recognizing human eyes," in *Geometric Methods in Computer Vision*, vol. 1570 of *Proceedings of SPIE*, pp. 214–226, San Diego, Calif, USA, July 1991.

[2] S. Amarnag, R. S. Kumaran, and J. N. Gowdy, "Real time eye tracking for human computer interfaces," in *Proceedings of the International Conference on Multimedia and Expo (ICME '03)*, vol. 3, pp. 557–560, Baltimore, Md, USA, July 2003.

[3] Q. Ji and X. Yang, "Real-time eye, gaze, and face pose tracking for monitoring driver vigilance," *Real-Time Imaging*, vol. 8, no. 5, pp. 357–377, 2002.

[4] P. Smith, M. Shah, and N. da Vitoria Lobo, "Monitoring head/eye motion for driver alertness with one camera," in *Proceedings of the 15th International Conference on Pattern Recognition (ICPR '00)*, vol. 4, pp. 636–642, Barcelona, Spain, September 2000.

[5] T. D'Orazio, M. Leo, P. Spagnolo, and C. Guaragnella, "A neural system for eye detection in a driver vigilance application," in *Proceedings of the 7th International IEEE Conference on Intelligent Transportation Systems (ITS '04)*, pp. 320–325, Washington, DC, USA, October 2004.

[6] K. F. Van Orden, T.-P. Jung, and S. Makeig, "Combined eye activity measures accurately estimate changes in sustained visual task performance," *Biological Psychology*, vol. 52, no. 3, pp. 221–240, 2000.

[7] R. Shaw, E. Crisman, A. Loomis, and Z. Laszewski, "The eye wink control interface: using the computer to provide the severely disabled with increased flexibility and comfort," in *Proceedings of the 3rd Annual IEEE Symposium on Computer-Based Medical Systems (CBMS '90)*, pp. 105–111, Chapel Hill, NC, USA, June 1990.

[8] L. Gan, B. Cui, and W. Wang, "Driver fatigue detection based on eye tracking," in *Proceedings of the 6th World Congress on Intelligent Control and Automation (WCICA '06)*, vol. 2, pp. 5341–5344, Dalian, China, June 2006.

[9] A. Haro, M. Flickner, and I. Essa, "Detecting and tracking eyes by using their physiological properties, dynamics, and appearance," in *Proceedings of the IEEE Conference on Computer Vision and Pattern Recognition (CVPR '00)*, vol. 1, pp. 163–168, Hilton Head Island, SC, USA, June 2000.

[10] A. Iijima, M. Haida, N. Ishikawa, H. Minamitani, and Y. Shinohara, "Head mounted goggle system with liquid crystal display for evaluation of eye tracking functions on neurological disease patients," in *Proceedings of the 25th Annual International Conference of the IEEE Engineering in Medicine and Biology Society (EMBS '03)*, vol. 4, pp. 3225–3228, Cancun, Mexico, September 2003.

[11] I. Fasel, B. Fortenberry, and J. Movellan, "A generative framework for real time object detection and classification," *Computer Vision and Image Understanding*, vol. 98, no. 1, pp. 182–210, 2005.

[12] Z. Zhu and Q. Ji, "Robust real-time eye detection and tracking under variable lighting conditions and various face orientations," *Computer Vision and Image Understanding*, vol. 98, no. 1, pp. 124–154, 2005.

[13] C. H. Morimoto and M. Flickner, "Real-time multiple face detection using active illumination," in *Proceedings of the 4th IEEE International Conference on Automatic Face and Gesture Recognition (FG '00)*, pp. 8–13, Grenoble, France, March 2000.

[14] X. Liu, F. Xu, and K. Fujimura, "Real-time eye detection and tracking for driver observation under various light conditions," in *Proceedings of the IEEE Intelligent Vehicle Symposium (IV '02)*, vol. 2, pp. 344–351, Versailles, France, June 2002.

[15] D. W. Hansen and A. E. C. Pece, "Eye tracking in the wild," *Computer Vision and Image Understanding*, vol. 98, no. 1, pp. 155–181, 2005.

[16] D. Chai and K. N. Ngan, "Face segmentation using skin-color map in videophone applications," *IEEE Transactions on Circuits and Systems for Video Technology*, vol. 9, no. 4, pp. 551–564, 1999.

[17] D. Chai, S. L. Phung, and A. Bouzerdoum, "Skin color detection for face localization in human-machine communications," in *Proceedings of the 6th International, Symposium on Signal Processing and Its Applications (ISSPA '01)*, vol. 1, pp. 343–346, Kuala Lumpur, Malaysia, August 2001.

[18] V. N. Vapnik, *The Nature of Statistical Learning Theory*, Springer, New York, NY, USA, 1995.
[19] N. Otsu, "A threshold selection method from gray-level histograms," *IEEE Transcations on Systems, Man, and Cybernetics*, vol. 9, no. 1, pp. 62–66, 1979.